PIEZOELECTRIC PUSHERS FOR ACTIVE VIBRATION CONTROL OF ROTATING MACHINERY

A.B. Palazzolo
Department of Mechanical Engineering
Texas A&M University
College Station, Texas 77843-3123, U.S.A.

A.F. Kascak
Propulsion Directorate
U.S. Army Aviation Research and Technology Activity - AVSCOM
Lewis Research Center, MS 23-3
Cleveland, Ohio 44135, U.S.A.

R.R. Lin
Department of Mechanical Engineering
Texas A&M University
College Station, Texas 77843-3123, U.S.A.

J. Montague
Sverdrup Technology
NASA Lewis Research Center Group
Cleveland, Ohio 44135, U.S.A.

R.M. Alexander
Department of Mechanical Engineering
Texas A&M University
College Station, Texas 77843-3123, U.S.A.

The active control of rotordynamic vibrations and stability by magnetic bearings and electromagnetic shakers has been discussed extensively in the literature. These devices, though effective, are usually large in volume and add significant weight to the stator. The use of piezoelectric pushers may provide similar degrees of effectiveness in light, compact packages. This paper contains analyses which extend quadratic regulator, pole placement and derivative feedback control methods to the "prescribed displacement" character of piezoelectric pushers. The structural stiffness of the pusher is also included in the theory.

Tests are currently being conducted at NASA Lewis Research Center with piezoelectric pusher-based active vibration control. The paper presents results performed on the NASA test rig as preliminary verification of the related theory.

NOMENCLATURE

$[A^{Dm}]$: Coefficient matrix associated with $\{X\}$ in state space

$[B_F^{Dm}]$: Coefficient matrix associated with $\{F_D\}$ in state space

$[B_U^{Dm}]$: Coefficient matrix associated with $\{U\}$ in state space

$[C]$: Damping matrix

$[\tilde{C}]$: Uncoupled velocity feedback damping matrix

C_i^A : Feedback positive active damping

$[C_F]$: Feedback damping matrix

C_s : Damping coef. of the piezoelectric stack

$[C_S]$: Coef. matrix associated with the output vector

e_1 : Eccentricity

F_i : Imbalance forces due to mass imbalance

$\{F_D(t)\}$: External forces (disturbance)

F_{P_i} : Force produced by the i^{th} pusher

$[G']$: System gain matrix

[I] : Identity (unity) matrix

I_P : Polar moment of inertia

I_T : Moment of inertia

min J : Minimize the performance index J

[K] : Stiffness matrix

$[K^D]$: Stiffness matrix including the pusher stiffness

$[K^{DD}]$: Pusher stiffness matrix

$[K_F]$: Feedback stiffness matrix

K_p : Preload spring inside the pusher

K_s : Stiffness of the stack of piezoelectric discs

M : Number of piezoelectric pushers

[M] : Mass matrix

N : Number of degrees of freedom

[P] : Matrix solution from Riccati equation

[Q] : Weighting matrix associated with state vector

r : Number of observer's output

[R] : Weighting matrix associated with control vector

t : Number of modes used

$\{U\}$: Control force matrix

$\{X\}$: State vector

$\{Y\}$: Output vector

$\{Z\}$: Space coordinates

Z_i^* : Pusher tip displacement

$\{\alpha\}$: Prescribed displacement of the pushers

ζ_i : i^{th} modal damping

$\{\xi\}$: Modal coordinates

$[\Phi^D]$: Mode shape matrix

$[\Phi]^T$: Transpose matrix of mode shape matrix

$[\Omega_i]$: i^{th} natural frequency

[diag( )] : Diagonal matrix

INTRODUCTION

An increasing amount of research is being devoted to developing effective active vibration control packages for rotating machinery, machine tools, large space structures, and in robotics. The advantages of active control over passive, i.e., absorbers and dampers, is the versatility of active control in adjusting to a myriad of load conditions and machinery configurations. This is clearly illustrated when one considers the very narrow bandwidth that a tuned spring mass absorber is effective in.

Electromagnetic shakers and magnetic bearings have been used for actuators in the majority of the active vibration control research mentioned in the literature. Schweitzer (1985) examined the stability and observability of rotor bearing systems with active vibration control, and

C-2

presented an analysis which related force and stiffness to electrical and geometrical properties of electromagnetic bearings.

Nikolajsen (1979) examined the application of magnetic dampers to a 3.2 meter simulated marine propulsion system. Gondholekar and Holmes (1984) suggested that electromagnetic bearings be employed to shift critical speeds by altering the suspension stiffness. Weise (1985) discussed proportional, integral, derivative (PID) control of rotor vibrations and illustrated how magnetic bearings could be used to balance a rotor by forcing it to spin about it's inertial axis. Humphris et al. (1986) compared predicted and measured stiffness and damping coefficients for a magnetic journal bearing.

Several papers describe active vibration control utilizing other types of actuators. Feng (1986) developed an active vibration control scheme with actuator forces resulting from varying bearing oil pressure. Heinzmann (1980) employed loud speaker coils linked to the shaft via ball bearings, to control vibrations.

This paper develops theory and shows test results corresponding to incorporating piezoelectric pushers as actuator devices for active vibration control. The usual application for these devices is for obtaining minute position adjustments of lenses and mirrors in laser systems (Burleigh, 1986). In the proposed application the pushers force the squirrel cage - ball bearing supports of a rotating shaft. The induced vibration counteracts the unbalanced vibration of the shaft by contributing active damping to the system. The paper presents active vibration control theory and test results for the piezoelectric pushers. To the authors'knowledge this represents a new application of piezoelectric actuators although there has been previous applications to the bending vibration of non-rotating beams using layered piezoelectric materials (Tzou, 1987).

THEORY

The piezoelectric pushers consist of a stack of piezoelectric ceramic discs which are arranged on top of one another and connected in parallel electrically. The stack expands in response to an applied voltage which causes the electric field to point in the direction of polarization for each disc. The extension of the pusher depends on the number and thickness of the discs and

the force depends on the cross sectional area of the discs. Figure 1 shows a sketch of a pusher and the corresponding ideal model. The model consists of a prescribed displacement (α) which is proportional to the input voltage and a spring (K_s) representing the stiffness of the stack of piezoelectric discs. The stiffness K_p is a preload spring which is typically 0.001 to 0.01 times the stiffness K_s. The figure shows that the device has a bilinear spring unless the tip is sufficient ly preloaded to maintain a zero gap at all times. The model utilized in the upcoming analysis neglects nonlinearities in the electrical and structural characteristics of the devices and damping (C_s) in the piezoelectric stack.

If pushers are attached to m distinct degrees of freedom of the model, it's matrix differential equation may be partitioned and rearranged into the form,

$$[M]_{(N\times N)}\{\ddot{Z}\}_{(N\times 1)} + [C]_{(N\times N)}\{\dot{Z}\}_{(N\times 1)} + [K^D]_{(N\times N)}\{Z\}_{(N\times 1)} = \{F_D(t)\}_{(N\times 1)} - [K^{DD}]_{(N\times M)}\{\alpha\}_{(M\times 1)} \tag{1}$$

where N and M are the number of degrees of freedom of the rotor and the number of piezoelectric pushers, respectively, and

$$[K^D]_{(N\times N)} = [K]_{(N\times N)} + \begin{pmatrix} \cdots & \vdots & \cdots & \vdots & \cdots & \vdots & \cdots \\ \cdots & k_1 & \cdots & \vdots & \cdots & \vdots & \cdots \\ \cdots & \vdots & \cdots & k_2 & \cdots & \vdots & \cdots \\ \cdots & \vdots & \cdots & \vdots & \ddots & \vdots & \cdots \\ \cdots & \vdots & \cdots & \vdots & \cdots & k_m & \cdots \\ \cdots & \vdots & \cdots & \vdots & \cdots & \vdots & \cdots \end{pmatrix} \tag{2}$$

$$[K^{DD}]_{(N\times M)} = -\begin{pmatrix} \cdots & \cdots & \cdots & \cdots \\ k_1 & \cdots & \cdots & \cdots \\ \cdots & k_2 & \cdots & \cdots \\ & & \ddots & \\ \cdots & \cdots & \cdots & k_m \\ \cdots & \cdots & \cdots & \cdots \end{pmatrix} \tag{3}$$

and

$$\{\alpha\} = \begin{pmatrix} \alpha_1 \\ \alpha_2 \\ \vdots \\ \alpha_m \end{pmatrix} \tag{4}$$

The matrices [M], [C], and [K] are the mass, damping,and stiffness matrices of the rotor bearing system without the pushers installed, as defined in (Palazzolo, 1983). The K_i are the effective stiffness of the pushers, which from Figure 1 are $K_i = (1/K_{si} + 1/K_{pi})^{-1}$. The stiffness K_i is inserted at the degree of freedom whose motion is the same as the tip motion of the corresponding pusher. The parameter α_i is the prescribed internal displacement of pusher i, which is assumed to vary linearly with input voltage.

The following portions of the paper provide the mathematical means for incorporating the piezoelectric pusher model into three standard active vibration control algorithms.

Part I: Optimal Control

Define the modal transformation

$$\{Z\}_{(N\times 1)} = [\Phi^D]_{(N\times t)}\{\xi\}_{(t\times 1)} \tag{5}$$

where t is the number of modes used in the modal space and $[\Phi^D]$ is the mode shape matrix for the system that includes the pusher stiffness. Substitute Eq.(5) into Eq.(1) and premultiply by $[\Phi^D]^T$, the transpose matrix of $[\Phi^D]$. Furthermore, assume that the system is proportionately damped, and the mass matrix has been orthonormalized;

$$[\Phi^D]^T[M][\Phi^D] = [I]_{(t\times t)} \tag{6}$$

Then, from the orthogonality conditions, Eq.(1) can be expressed as

$$\{\ddot{\xi}\} + [diag(2\zeta_i^D\Omega_i^D)]\{\dot{\xi}\} + [diag([\Omega_i^D]^2)]\{\xi\} = [\Phi^D]^T\{F_D\} - [\Phi^D]^T[K^{DD}]\{\alpha\} \tag{7}$$

Eq.(7) can be written as a first order (state space) form by adding an identity equation as follows.

$$\begin{pmatrix} [I_t] & \vdots & [0] \\ \cdots & \cdots & \cdots \\ [0] & \vdots & [diag(-(\Omega_i^D)^2)] \end{pmatrix} \begin{pmatrix} \{\ddot{\xi}\} \\ \cdots \\ \{\dot{\xi}\} \end{pmatrix} + \begin{pmatrix} [diag(2\zeta_i^D\Omega_i^D)] & \vdots & [diag((\Omega_i^D)^2)] \\ \cdots & \cdots & \cdots \\ [diag((\Omega_i^D)^2)] & \vdots & [0] \end{pmatrix} \begin{pmatrix} \{\dot{\xi}\} \\ \cdots \\ \{\xi\} \end{pmatrix}$$
$$= \begin{pmatrix} [\Phi^D]^T\{F_D\} \\ \cdots \\ [0] \end{pmatrix} + \begin{pmatrix} -[\Phi^D]^T[K^{DD}]\{\alpha\} \\ \cdots \\ [0] \end{pmatrix} \tag{8}$$

Multiplying Eq.(8) by the inverse of the leading coefficient matrix yields

$$\{\dot{X}^m\}_{(2t\times 1)} = [A^{Dm}]_{(2t\times 2t)}\{X^m\}_{(2t\times 1)} + [B_F^{Dm}]_{(2t\times N)}\{F_D\}_{(N\times 1)} + [B_U^{Dm}]_{(2t\times M)}\{\alpha\}_{(M\times 1)} \tag{9}$$

where

$$[A^{Dm}]_{(2t\times 2t)} = \begin{pmatrix} [diag(-2\zeta_i^D\Omega_i^D)] & \vdots & [diag(-(\Omega_i^D)^2)] \\ \cdots & \cdots & \cdots \\ [I_t] & \vdots & [0] \end{pmatrix} \tag{10}$$

$$[B_F^{Dm}]_{(2t\times N)} = \begin{pmatrix} [\Phi^D]^T \\ \cdots \\ [0] \end{pmatrix} \tag{11}$$

$$[B_U^{Dm}]_{(2t\times M)} = \begin{pmatrix} -[\Phi^D]^T[K^{DD}] \\ \cdots \\ [0] \end{pmatrix} \tag{12}$$

$$\{X\}_{(2t\times 1)} = \begin{pmatrix} \{\dot{\xi}\} \\ \cdots \\ \{\xi\} \end{pmatrix} \tag{13}$$

Since it is impractical to measure the displacement and velocity at all the system degrees of freedom (dof), an observer system may be constructed to estimate the state vector from a smaller number of measurements. This approach, however, may not be feasible for a large rotordynamic system involving many degrees of freedom and excitation at high frequencies. Another approach is output feedback, i.e., limit the control measurements to only those defined in the output vector, $\{Y\}$, defined by

$$\{Y\}_{(r\times 1)} = [C_S]_{(r\times 2N)}\begin{pmatrix} \{\dot{Z}\} \\ \cdots \\ \{Z\} \end{pmatrix}_{(2N\times 1)} \tag{14}$$

The control for the prescribed "internal" displacements of the pushers is

$$\{\alpha\}_{(M\times 1)} = -[G']_{(M\times r)}\{Y\}_{(r\times 1)} \tag{15}$$

where r is the number of sensors (velocities and displacements), and M the number of pushers. Substituting Eq.(14) in Eq.(15) and converting this equation to the modal space with Eq.(5) yields

$$\{\alpha\}_{(M\times 1)} = -[G'][C_S] \begin{pmatrix} [\Phi^D] & \vdots & [0] \\ \dots & \dots & \dots \\ [0] & \vdots & [\Phi^D] \end{pmatrix} \begin{pmatrix} \{\dot{\xi}\} \\ \dots \\ \{\xi\} \end{pmatrix} \tag{16}$$

or in abbreviated notation

$$\{\alpha\}_{(M\times 1)} = -[\tilde{G}]_{(M\times 2t)}\{X\}_{(2t\times 1)} \tag{17}$$

where

$$[\tilde{G}]_{(M\times 2t)} = [G']_{(M\times r)}[C_S]_{(r\times 2N)} \begin{pmatrix} [\Phi^D] & \vdots & [0] \\ \dots & \dots & \dots \\ [0] & \vdots & [\Phi^D] \end{pmatrix}_{(2N\times 2t)} \tag{18}$$

The objective of output feedback control in modal space can now be identified as obtaining the gain matrix $[G']$ in Eq.(15) that suppresses the modal coordinates ξ_i in Eq.(5). The linear quadratic regulator problem goes one step further and also simultaneously reduces the required control displacements $\{\alpha_i\}$. The performance index to be minimized is defined as

$$min_{\{\alpha\}}\ J = min_{\{\alpha\}} \int_0^\infty (\{X\}^T[Q]\{X\} + \{\alpha\}^T[R]\{\alpha\})dt \tag{19}$$

where [Q] and [R] are symmetric, positive-definite weighting matrices which govern the relative importance of minimizing the modal coordinates ξ_i and the prescribed pusher displacements, α_k. Diminishing [R] will result in larger pusher "internal" displacements but smaller vibrations (governed by the ξ_i). Optimal control theory produces the solution for Eq.(19) in the form of Eq.(17). The gain matrix $[\tilde{G}]$ is computed from

$$[\tilde{G}]_{(M\times 2t)} = [R]^{-1}_{(M\times M)}[B_U^{Dm}]^T_{(M\times 2t)}[P]_{(2t\times 2t)} \tag{20}$$

where [P] is obtained as the solution matrix to the algebraic (steady state) Ricatti equation (Palazzolo, 1988). The steady state (algebraic) Ricatti equation is

$$[P][A^{Dm}] + [A^{Dm}]^T[P] - [P][B_U^{Dm}][R]^{-1}[B_U^{Dm}]^T[P] + [Q] = [0]_{(2t\times 2t)} \tag{21}$$

where the matrices [P], $[A^{Dm}]$, and [Q] are 2t by 2t, the matrix $[B_U^{Dm}]$ is 2t by M, and the matrix [R] is M by M.

If Eq.(18) is to be solved exactly for G', the number of measured outputs r (sum of velocities and displacements) must equal twice the number of modes, t, used in the modal space. Define the matrix $[\beta]$ as

$$[\beta]_{(r\times 2t)} = [C_S]_{(r\times 2N)} \begin{pmatrix} [\Phi^D] & \vdots & [0] \\ \cdots & \cdots & \cdots \\ [0] & \vdots & [\Phi^D] \end{pmatrix}_{(2N\times 2t)} \tag{22}$$

Assuming that r=2t and $[\beta]$ is nonsingular, the gain matrix $[G']$ can be derived from Eq.(18) and Eq.(20) as

$$[G'] = [R]^{-1}[B_U^{Dm}]^T[P][\beta]^{-1} \tag{23}$$

The prescribed "internal" displacement of the i^{th} pusher can now be expressed from Eq.(15) and Eq.(23) as

$$\alpha_i = -\sum_{j=1}^{r} G'_{ij} y_j \tag{24}$$

The force produced by the i^{th} pusher is

$$F_{P_i} = k_i(Z_i^* - \alpha_i) \tag{25}$$

where Z_i^* is the pusher tip displacement. Substituting Eq.(14) and Eq.(15) into Eq.(1) yields

$$\begin{aligned} &[M]_{(N\times N)}\{\ddot{Z}\}_{(N\times 1)} + [C]_{(N\times N)}\{\dot{Z}\}_{(N\times 1)} + [K^D]_{(N\times N)}\{Z\}_{(N\times 1)} = \\ &\{F_D(t)\}_{(N\times 1)} + [K^{DD}]_{(N\times M)}[G']_{(M\times r)}[C_S]_{(r\times 2N)} \begin{pmatrix} \{\dot{Z}\} \\ \cdots \\ \{Z\} \end{pmatrix}_{(2N\times 1)} = \\ &\{F_D(t)\}_{(N\times 1)} + [C_F]_{(N\times N)}\{\dot{Z}\}_{(N\times 1)} + [K_F]_{(N\times N)}\{Z\}_{(N\times 1)} \end{aligned} \tag{26}$$

where

$$\left[[C_F]_{(N\times N)} \vdots [K_F]_{(N\times N)}\right] = [K^{DD}][G'][C_S] \tag{27}$$

Thus, the closed loop equilibrium equation becomes

$$[M]_{(N\times N)}\{\ddot{Z}\}_{(N\times 1)} + [[C] - [C_F]]_{(N\times N)}\{\dot{Z}\}_{(N\times 1)} + [[K^D] - [K_F]]_{(N\times N)}\{Z\}_{(N\times 1)} = \{F_D(t)\}_{(N\times 1)} \tag{28}$$

This equation is very useful for conducting rotordynamic simulations with feedback control utilizing piezoelectric pushers.

Part II: Pole Placement

Similar to optimal control, Eq.(1) can be written in first order (state space) form as

$$\begin{pmatrix} [M] & \vdots & [0] \\ \cdots & \cdots & \cdots \\ [0] & \vdots & [-K^D] \end{pmatrix} \begin{pmatrix} \{\ddot{Z}\} \\ \cdots \\ \{\dot{Z}\} \end{pmatrix} + \begin{pmatrix} [C] & \vdots & [K^D] \\ \cdots & \cdots & \cdots \\ [K^D] & \vdots & [0] \end{pmatrix} \begin{pmatrix} \{\dot{Z}\} \\ \cdots \\ \{Z\} \end{pmatrix} = \begin{pmatrix} [F_D(t)] \\ \cdots \\ [0] \end{pmatrix} + \begin{pmatrix} [-K^{DD}] \\ \cdots \\ [0] \end{pmatrix} \{\alpha\} \tag{29}$$

Premultiplication by the inverse of the leading coefficient matrix yields

$$\begin{pmatrix} \{\ddot{Z}\} \\ \cdots \\ \{\dot{Z}\} \end{pmatrix} = \begin{pmatrix} [-[M]^{-1}[C]] & \vdots & [-[M^{-1}][K^D]] \\ \cdots & \cdots & \cdots \\ [I_N] & \vdots & [0] \end{pmatrix} \begin{pmatrix} \{\dot{Z}\} \\ \cdots \\ \{Z\} \end{pmatrix} + \begin{pmatrix} [M]^{-1} \\ \cdots \\ [0] \end{pmatrix} \{F_D\} + \begin{pmatrix} -[M]^{-1}[K^{DD}] \\ \cdots \\ [0] \end{pmatrix} \{\alpha\} \tag{30}$$

This equation is written in abbreviated notation as

$$\{\dot{X}\}_{(2N\times 1)} = [A^D]_{(2N\times 2N)}\{X\}_{(2N\times 1)} + [B_F^D]_{(2N\times N)}\{F_D\}_{(N\times 1)} + [B_\alpha]_{(2N\times M)}\{\alpha\}_{(M\times 1)} \tag{31}$$

where

$$\{X\}_{(2N\times 1)} = \begin{pmatrix} \{\dot{Z}\} \\ \cdots \\ \{Z\} \end{pmatrix} \tag{32}$$

The output vector, $\{Y\}$, and the output feedback control displacement, $\{\alpha\}$, have the same definitions as in Eq.(14) and Eq.(15), respectively. Substituting Eq.(14) into Eq.(15) yields

$$\{\alpha\}_{(M\times 1)} = -[G']_{(M\times r)}[C_S]_{(r\times 2N)}\{X\}_{(2N\times 1)} \tag{33}$$

Substitute Eq.(33) into Eq.(31) and rearrange

$$\{\dot{X}\} = ([A^D] - [B_\alpha][G'][C_S])\{X\} + [B_F^D]\{F_D\} \tag{34}$$

Consider the unforced system with

$$\{F_D\} = \{0\} \quad \& \quad \{X\} = [\Psi]e^{\lambda t} \tag{35}$$

The characteristic equation for the closed loop system becomes

$$\det(\lambda[I]_{(2N\times 2N)} - [A^D]_{(2N\times 2N)} + [B_\alpha]_{(2N\times M)}[G']_{(M\times r)}[C_S]_{(r\times 2N)}) = 0 \tag{36}$$

Assume that λ is not an eigenvalue of the open loop system, then Eq.(36) can be rewritten as

$$\det(\lambda[I_{2N}] - [A^D])_{(2N\times 2N)} \det([I]_{(2N\times 2N)} + \{\lambda[I_{2N}] - [A^D]\}^{-1}_{(2N\times 2N)}$$
$$[B_\alpha]_{(2N\times M)}[G']_{(M\times r)}[C_S]_{(r\times 2N)}) = 0 \tag{37}$$

Apply the following determinant identity (Brogan,1974)

$$\det([I_{2N}] + [PP]_{(2N\times M)}[QQ]_{(M\times 2N)}) = \det([I_M] + [QQ]_{(M\times 2N)}[PP]_{(2N\times M)}) \tag{38}$$

to Eq.(37) which then implies

$$\det([I_M] + [G']_{(M\times r)}[C_S]_{(r\times 2N)}\{\lambda[I_{2N}] - [A^D]\}^{-1}_{(2N\times 2N)}[B_\alpha]_{(2N\times M)}) = 0 \tag{39}$$

Define

$$[\Phi(\lambda)]_{(2N\times 2N)} = \{\lambda[I_{2N}] - [A^D]\}^{-1}_{(2N\times 2N)} \tag{40}$$

and

$$[\Psi(\lambda)]_{(r\times M)} = [C_S]_{(r\times 2N)}[\Phi(\lambda)]_{(2N\times 2N)}[B_\alpha]_{(2N\times M)} \tag{41}$$

Therefore, Eq.(39) becomes

$$\det([I_M] + [G']_{(M\times r)}[\Psi(\lambda)]_{(r\times M)}) = 0 \tag{42}$$

Eq.(42) implies that the solution will be satisfied if the column vectors of

$$[I_M] + [G'][\Psi(\lambda)] \tag{43}$$

are linearly dependent. Following (Fahmy, 1982) and (Stanway, 1984) this condition is expressed by

$$([I_M] + [G'][\Psi(\lambda_i)])\,\{f_i\}_{(M\times 1)} = \{0\}_{(M\times 1)} \tag{44}$$

for some $\{f_i\} \in \mathbf{R^m}$. For r prescribed values of λ, Eq.(44) can be expressed as

$$[f_1 \vdots f_2 \vdots \cdots \vdots f_r]_{(M\times r)} + [G'][\Psi(\lambda_1)f_1 \vdots \cdots \vdots \Psi(\lambda_r)f_r]_{(r\times r)} = [0]_{(M\times r)} \tag{45}$$

or in abbreviated notation,

$$[L]_{(M\times r)} + [G'][W]_{(r\times r)} = [0]_{(r\times r)} \tag{46}$$

The output feedback gain matrix is obtained from

$$[G'] = -[L]_{(M\times r)}[W]^{-1}_{(r\times r)} \tag{47}$$

Note that r poles have to be assigned to compute the matrix inverse $[W]^{-1}$. Eq.(47) provides the gain matrix for prescribing r eigenvalues where r is the total number of sensor measurements including velocities and displacements.

Physically, the gain matrix $[G']$ should be a real matrix, thus for each prescribed complex eigenvalue λ_i the complex conjugate λ_{i+1} should be prescribed too. In this case, set $\{f_{i+1}\} = \{f_i\}$

or let both $\{f_i\}$ and $\{f_{i+1}\}$ be real vectors. This implies that $\frac{r}{2}$ complex eigenvalue pairs $(\lambda_i, \lambda_{i+1})$ may be prescribed.

The pusher internal displacements are again obtained from Eq.(24). Furthermore, the feedback equivalent damping and stiffness matrices are exactly those shown in Eq.(27) and Eq.(28).

Part III: Uncoupled Velocity Feedback Damper

This is the simplest vibration control scheme in that it only involves the internal displacement of the pusher and the velocity of it's tip. If the tip of the i^{th} pusher is in constant contact with the l_i degree of freedom, the control law becomes

$$\alpha_i = -G'_{ii}\dot{Z}_{l_i}, \quad i = 1, 2, \ldots, m \tag{48}$$

Then

$$[K^{DD}]\{\alpha\} = \begin{pmatrix} 0 \\ \vdots \\ k_1\alpha_1 \\ 0 \\ \vdots \\ k_m\alpha_m \\ 0 \\ \vdots \\ 0 \end{pmatrix} = \begin{pmatrix} 0 \\ \vdots \\ 0 \\ -k_1G'_{11} \\ 0 \\ \vdots \\ \vdots \\ 0 \end{pmatrix} \dot{z}_1 + \ldots + \begin{pmatrix} 0 \\ \vdots \\ \vdots \\ \vdots \\ 0 \\ -k_mG'_{mm} \\ 0 \\ 0 \end{pmatrix} \dot{z}_m \tag{49}$$

Substitution of Eq.(49) into Eq.(1) produces the closed loop equilibrium equation;

$$[M]_{(N\times N)}\{\ddot{Z}\}_{(N\times 1)} + [\tilde{C}]_{(N\times N)}\{\dot{Z}\}_{(N\times 1)} + [K^D]_{(N\times N)}\{Z\}_{(N\times 1)} = \{F_D(t)\}_{(N\times 1)} \tag{50}$$

where

$$[\tilde{C}] = [C] + \begin{pmatrix} \ldots & \vdots & \ldots & \vdots & \ldots & \vdots & \ldots \\ \ldots & C_1^A & \ldots & \vdots & \ldots & \vdots & \ldots \\ \ldots & \vdots & \ldots & C_2^A & \ldots & \vdots & \ldots \\ \ldots & \vdots & \ldots & \vdots & \ddots & \vdots & \ldots \\ \ldots & \vdots & \ldots & \vdots & \ldots & C_m^A & \ldots \\ \ldots & \vdots & \ldots & \vdots & \ldots & \vdots & \ldots \end{pmatrix} \tag{51}$$

and

$$C_i^A = -k_i G'_{ii}, \quad i = 1, 2, \ldots, m \tag{52}$$

Eq.(52) shows how positive active damping may be added into the rotor bearing system via the simple control law in Eq.(48).

EXPERIMENTAL RESULTS

An air turbine driven rotor rig was instrumented to check the Uncoupled Velocity Feedback Damper theory described in the previous section. The piezoelectric actuators utilized in the tests were Burleigh Pusher PZL-100's, being driven by Burleigh PZ-150/150M Amplifier Drivers. Figure 2 shows a typical voltage vs. tip displacement plot for this arrangement. The curve in this plot provides an approximate description of the internal displacement (α) vs. voltage relation, since the tip is unloaded and the preload spring in Figure 1 is very light ($\simeq$ 20,000 N/M). Therefore it is assumed that the voltage sensitivity for α is S_A=-57,000.0 V/M. This value was nearly constant for the three pushers that were tested.

Load deflection characteristics of the pushers were obtained by securing each one in a solid cylinder, applying load to the protruding tip of the pusher, and measuring the tip deflections shown in Figure 3. Repeated tests with 3 separate pushers yielded an average stiffness of approximately 3.5×10^6 N/M.

Figure 4 shows a simple sketch of the test rig, which consists of a 2.5 cm diameter shaft, 61.0 cm in length; a 14.0 N overhung disc, 13.0 cm in diameter; and two squirrel cage mounted ball bearings. The outboard bearing is externally forced by an orthogonal pair of piezoelectric pushers, which are in turn positioned opposite to the two eddy current displacement probes d_3 and d_4. The control law in Eq.(48) applied to the test setup becomes

$$\alpha_{hor} = -G'_{hor} \ \dot{d}_4 \tag{53}$$

$$\alpha_{ver} = -G'_{ver} \ \dot{d}_3 \tag{54}$$

The horizontal and vertical active damping were set equal in the control arrangement of Figure 5. The figure outlines how an effective damping value can be computed once the probe and actuator sensitivities and actuator stiffness are known. The calculations for this test setup show that the "active" damping coefficient is estimated to vary according to

$$C_A = (275) \times G \frac{N\,sec}{M} \tag{55}$$

where G is the amplifier gain in Figure 5. The rotor was carefully balanced, and then intentionally unbalanced by a known amount (10.2 gm-cm), in order to compare the test results with those predicted by an unbalance response computer program.

Figure 6 and Figure 7 show the test vibration amplitude vs. speed plots for the disc probes d_1 and d_2 in Figure 4. The family of curves is generated by switching amplifier gains in Figure 5 and computing the effective damping according to Eq.(55). The computer simulation results for either probe d_1 or d_2, over the same range of damping values is shown in Figure 8. A comparison of Figures 6, 7 and 8 show that although the test damping is less than the predicted value from Eq.(55) a considerable amount of damping (10,000. N sec/M, 57 lb sec/in) is still produced.

Figure 9 and Figure 10 show the measured unbalanced response plots at the vertical (d_3) and horizontal (d_4) bearing probes, respectively. Figure 11 shows the theoretical response for the same probes. The results again indicate that Eq.(55) overpredicts the active damping, however by comparing the plots the pushers do provide approximately 14,000. N sec/M (80.0 lb sec/in) damping at the highest amplifier-gain setting.

The above comparison was also performed including gyroscopics in the theoretical model. This effect only caused minor changes in the predicted response.

SUMMARY AND CONCLUSIONS

This paper has examined the possible use of piezoelectric pushers for active control of rotor-bearing system vibrations. Although their most common application is currently micro-positioning of laser system mirrors and lenses; their stroke, force and frequency response make

them potentially very useful for vibration control. The obvious advantage of piezoelectric pushers over other actuators is their compact size and light weight.

Three active theories were extended to treat the special prescribed "internal" displacement (α) character of piezoelectric pushers. The Uncoupled Velocity-Feedback Damper theory was then tested by comparison to experimental results. The study showed that although the theory overpredicts the amount of damping produced by the pusher the actual level is significant, being in the range of 10,000-14,000. N sec/M (57.0-80.0 lb sec/in). The discrepancy between predicted and measured results most likely arises from the nonlinearity and hysteresis in the voltage-deflection and load-deflection characteristics of the pushers, and from the neglect of the structural damping of the piezoelectric stroke, by the theory. We are currently working with the pusher manufacturer, Burleigh Inc., to produce pushers that have reduced nonlinearity, hysteresis and stack damping. Construction of a feedback box to perform optimal control (OC) and pole placement control (PPC) is in progress. The device will accomodate up to 12 sensors and produce outputs to two actuators, which corresponds to a 2×12 dimension for the $[G']$ matrix in Eq.(15). Test results from application of OC and PPC will be forthcoming in the literature.

ACKNOWLEDGEMENTS

The authors wish to express their sincere gratitude for the following funding sources: NASA grant NAG3-763, ASEE-NASA Summer Faculty Fellowship Program,and the Texas A&M Turbomachinery Research Consortium (TRC). The invaluable assistance of the following people is also gratefully acknowledged: NASA (Tom Lokatos, Erwin Meyn, and John Ropchock) and Burleigh, Inc., (Dr. Jim Kaufer and Mark Palvino).

REFERENCES

Brogan, W.L. (1974) "Modern Control Theory," Quantum Publishers, Inc., New York, N.Y. 10010.

Burleigh Instruments (1986), Burleigh Park, Fishers, NY, 14453.

Fahmy, M.M. (1982) "On Eigenstructure Assignment in Linear Multivariable Systems," IEEE Trnas. on Automatic Control, Vol. AC-27, No. 3.

Feng, G., and Xin, N. (1986), "Automatic Control of the Vibration of the Flexible Rotor with Microcomputer," Int. Conf. on Rotordynamics, IFTOMM and JSME, Tokyo, Sept. pp.14-17.

Gondholekar, V., and Holmes, R. (1984), "Design of Electromagnetic Bearing for Vibration Control of Flexible Transmission Shaft," Rotor Dynamic Instability Problem in High Performance Turbomachinery, Texas A&M Univ., NASA report.

Heinzmann, J. et al. (1980), "The Implementation of Automatic Vibration Control in a High Speed Rotating Test Facility," Univ. of Virginia Report UVA/464761/MAE80/160.

Humphris, R., et al. (1986), "Effect of Control Algorithms on Magnetic Journal Bearing Properties," J. Eng. Gas Turbines and Power, ASME, Oct., Vol. 108, pp.624-632.

Nikolajsen, J., Holmes, R.,and Gondholekar, V. (1979), "Investigation of an Electromagnetic Damper for Vibration Control of a Transmission Shaft," Proc. Instn. Mech. Engr., Vol, 193, pp. 331-336.

Palazzolo, A.B., Wang, B.P., and Pilkey, W.D. (1983), "Eigensolution Reanalysis of Rotordynamic Systems by the Generalized Receptance Method," Jour. of Engin. for Power, Vol. 105, July, pp.543-550.

Palazzolo, A.B., Lin, R.R., Kascak, A.F., and Alexander, R.M. (1988), "Active Control of Transient Rotordynamic Vibration by Optimal Control Methods," Paper No. 88-GT-73, Presented at Gas Turbine Conf., June 5-9, 1988, Amsterdam, Accepted for publication (Jour. of Engr. for Gas Turbine and Power, April 1989).

Schweitzer, G. (1985) "Magnetic Bearings for Vibration Control," Bently Nevada Instability Seminar, Minden,Nevada. NASA CP-2409, p.317.

Stanway, R., and O'Reilly, C. (1984), "State Variable Feedback Control of Rotor Bearing Suspension Systems," Inst. Mech. Engr. Rotordynamics Conf. C274/84, pp.515-524.

Tzou, H.S. (1987), "Active Vibration Control of Flexible Structures Via Converse Piezoelec-

tricity," Presented at the 20th Midwestern Mechanics Conference, 8/31-9/2, 1987, Developments in Mechanics, pp.1201-1206, Vol. 14-c.

Weise, D., (1985), "Active Magnetic Bearings Provide Closed Loop Servo Control for Enhanced Dynamic Response," Proc. 27th IEEE Machine Tool Conf., October.

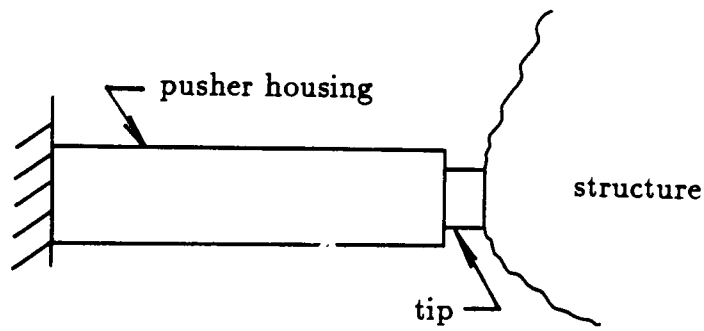

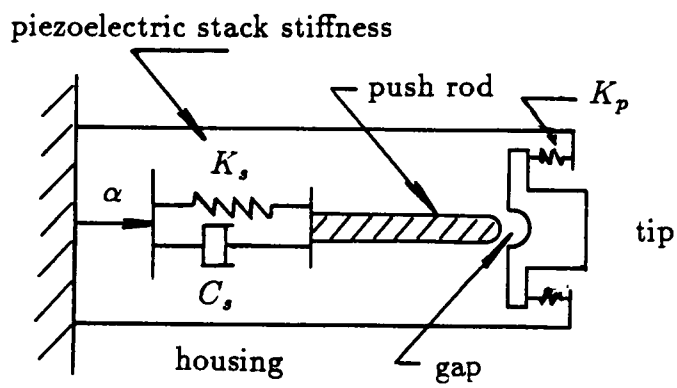

Figure 1 Sketch of piezoelectric pusher and corresponding analytical model.

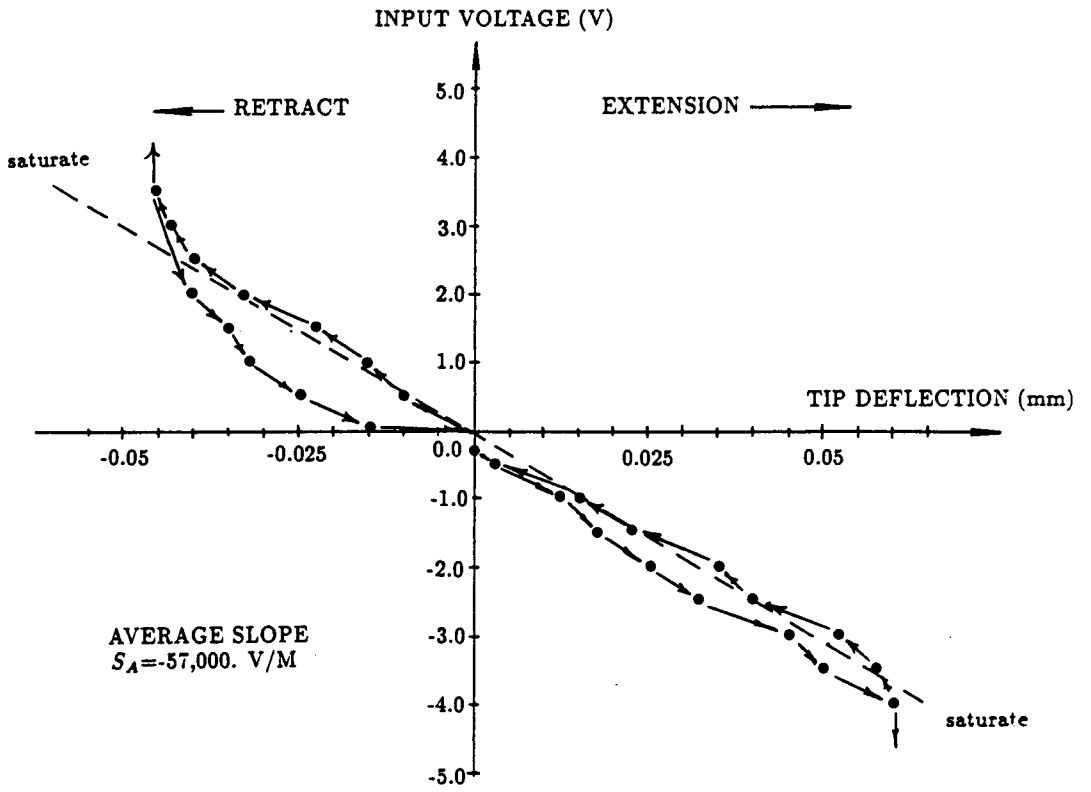

Figure 2 Typical pusher tip deflection vs. input voltage.

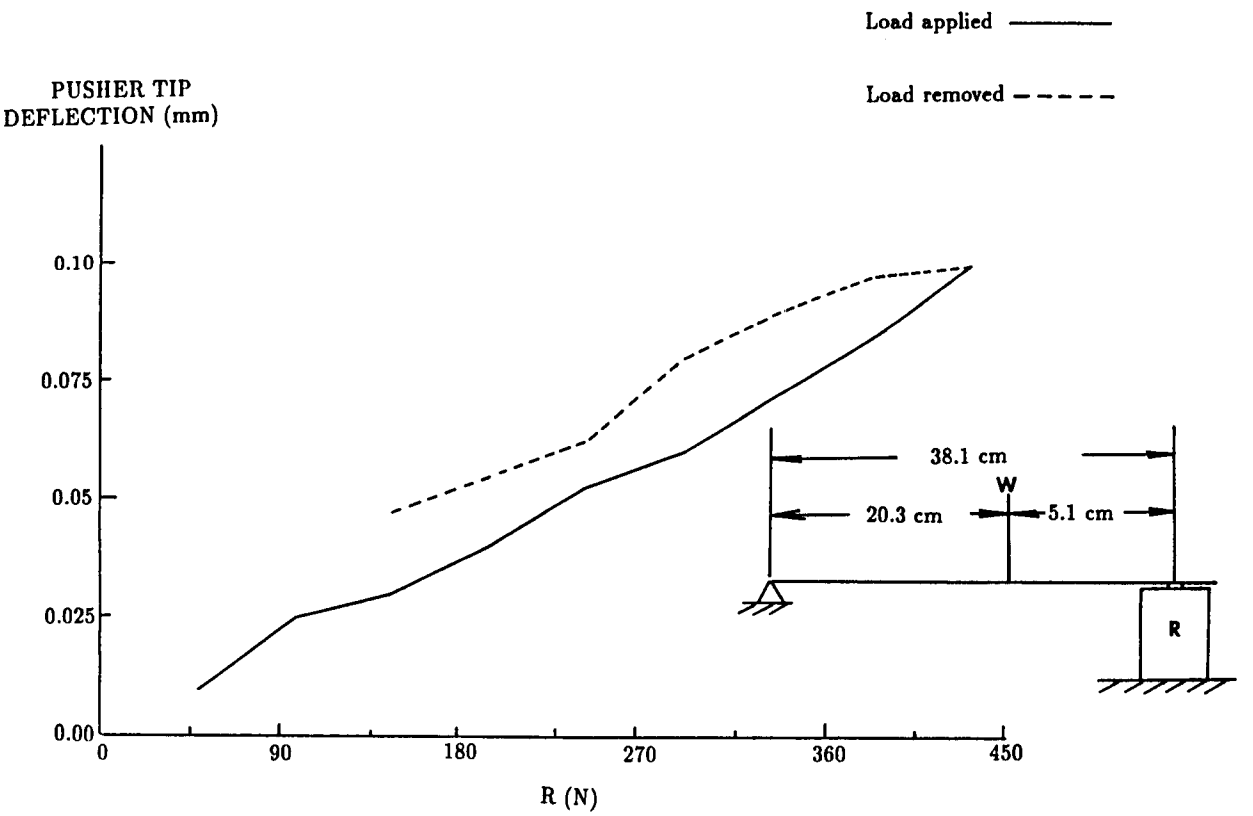

Figure 3 Typical pusher tip deflection vs. pusher tip load.

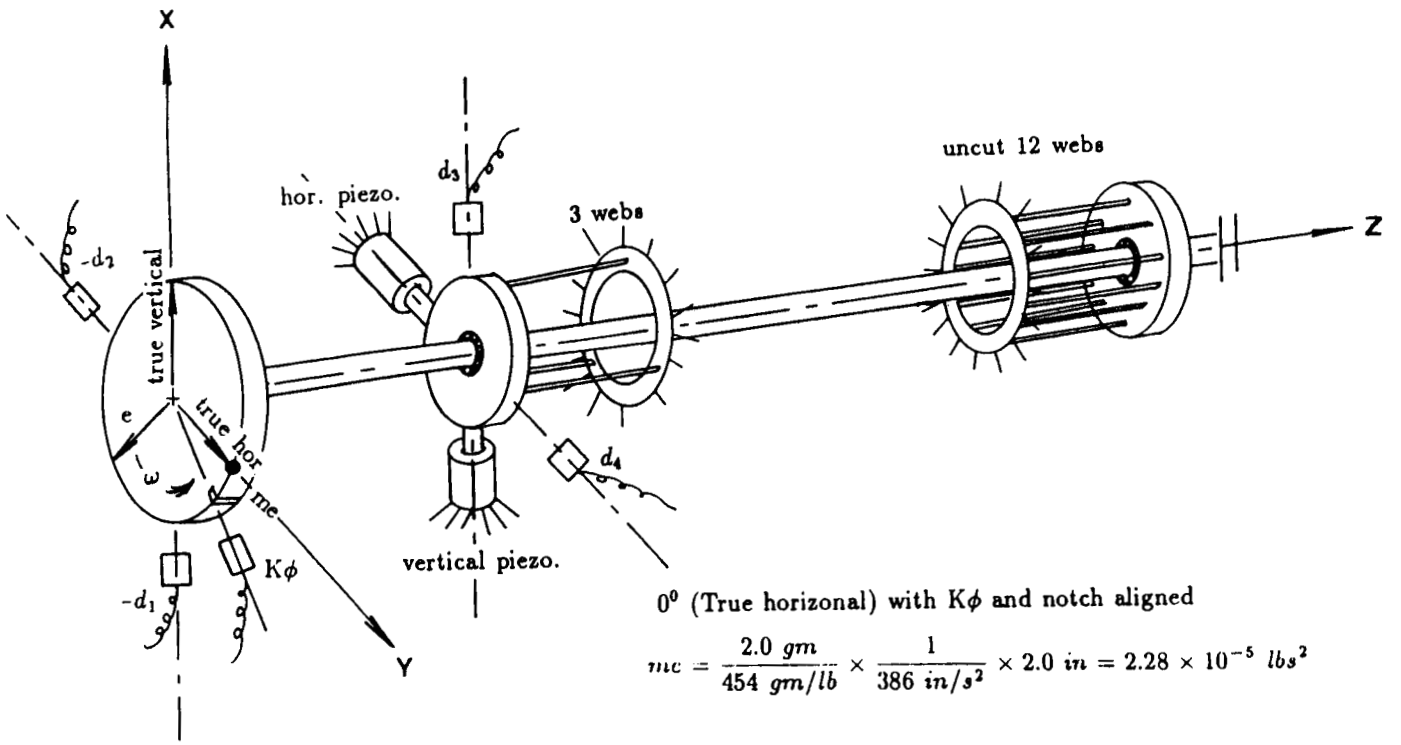

Figure 4 Diagram test rig with piezoelectric pushers.

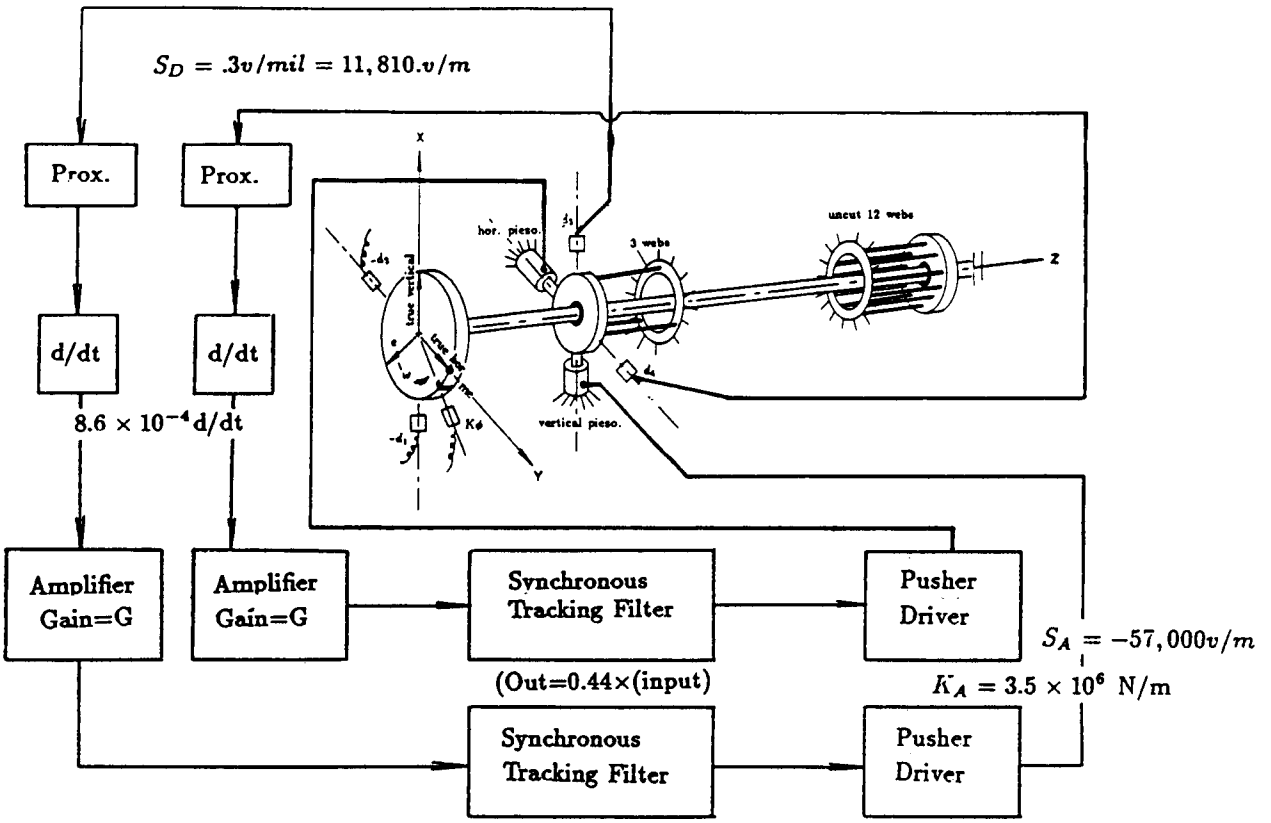

Uncoupled Velocity Feedback; $\alpha = G'\dot{d}$ (a)

Active Damping $C_A = K_A G'$ (b)

Actuator input voltage for α displacement, V_A, is

$$V_A = S_A \alpha_j \quad (c)$$

From (a) and substituting the data shown in Figure;

$$V_A = S_A G' \dot{d} = S_D(8.6 \times 10^{-4}\dot{d})G(0.44) \quad (d)$$

Thus

$$S_A \frac{C_A}{K_A}\dot{d} = S_D \times G(3.8 \times 10^{-4})\dot{d} \quad (e)$$

Or

$$C_A = 3.8 \times 10^{-4} \frac{S_D}{S_A} \times G \times K_A \times sec$$

Hence

$$C_A = (3.8 \times 10^{-4} sec)\frac{11,810v/m}{57,000v/m}(3.5 \times 10^6 N/m) \times G$$

$$= 275 \times G\frac{N sec}{m}\ (1.57 \times G\frac{lbsec}{in})$$

Figure 5 Outlines of system setup and the related equipment coefficients.

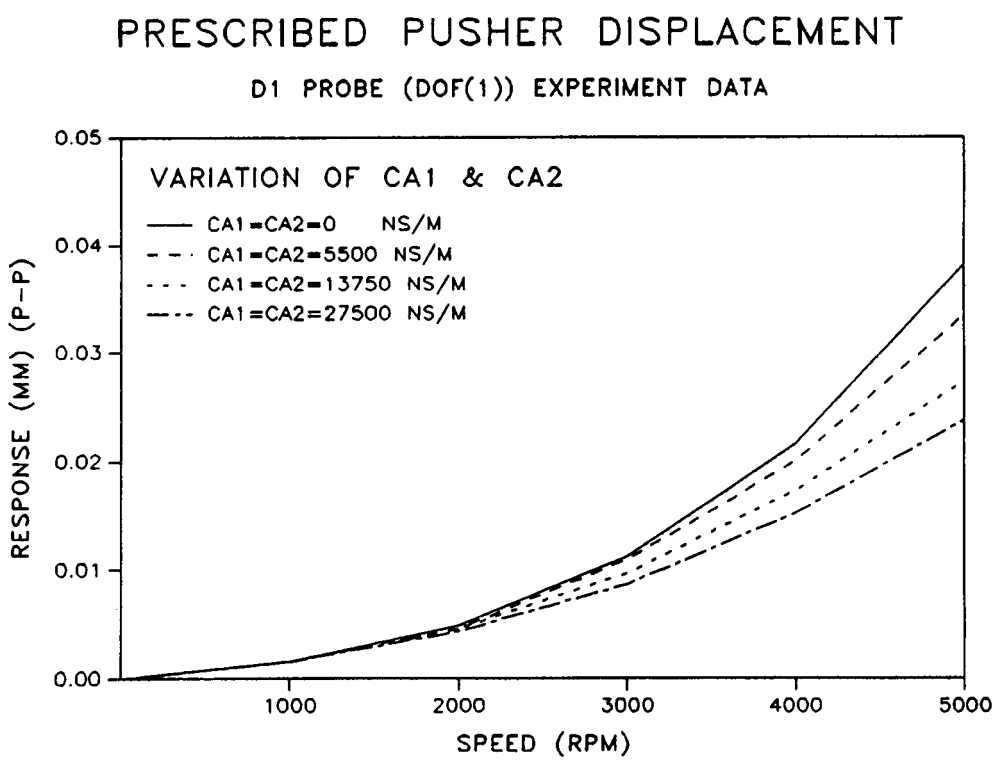

Figure 6 Prescribed pusher displacement at probe d_1 (DOF 1).

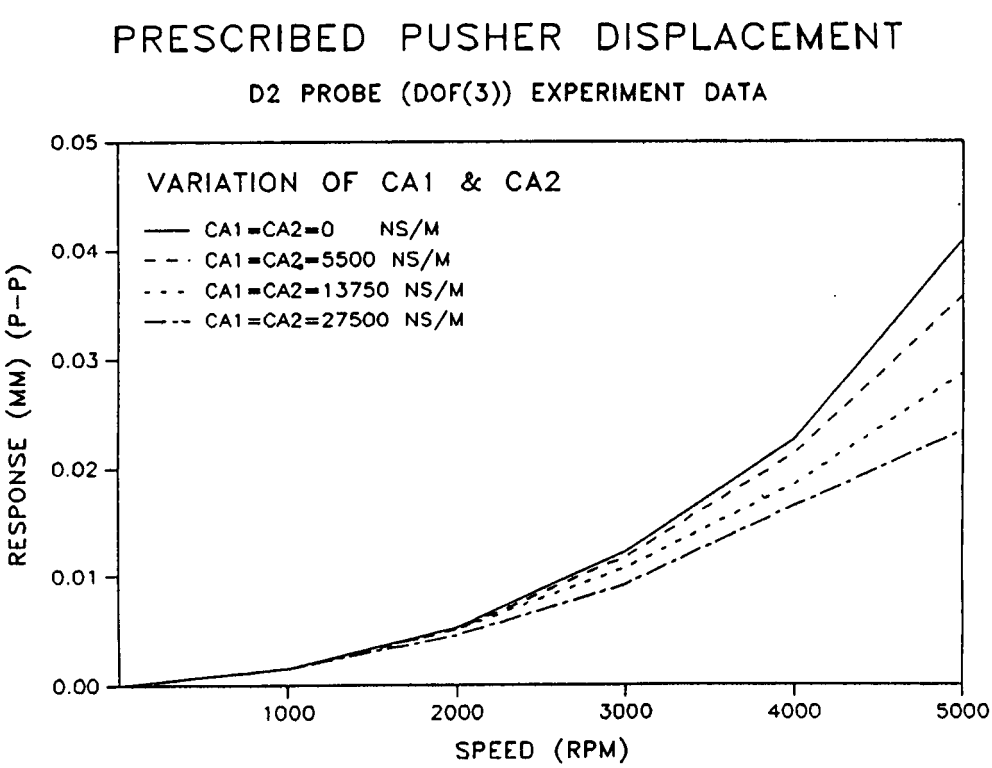

Figure 7 Prescribed pusher displacement at probe d_2 (DOF 3).

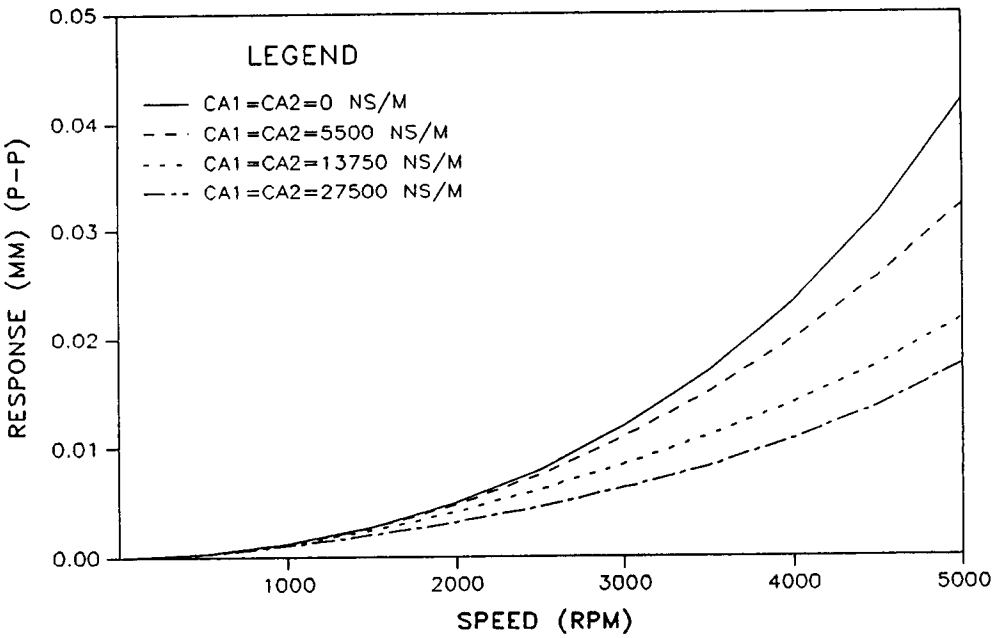

Figure 8 Computer simulation results of prescribed pusher displacement, d_1 probe.

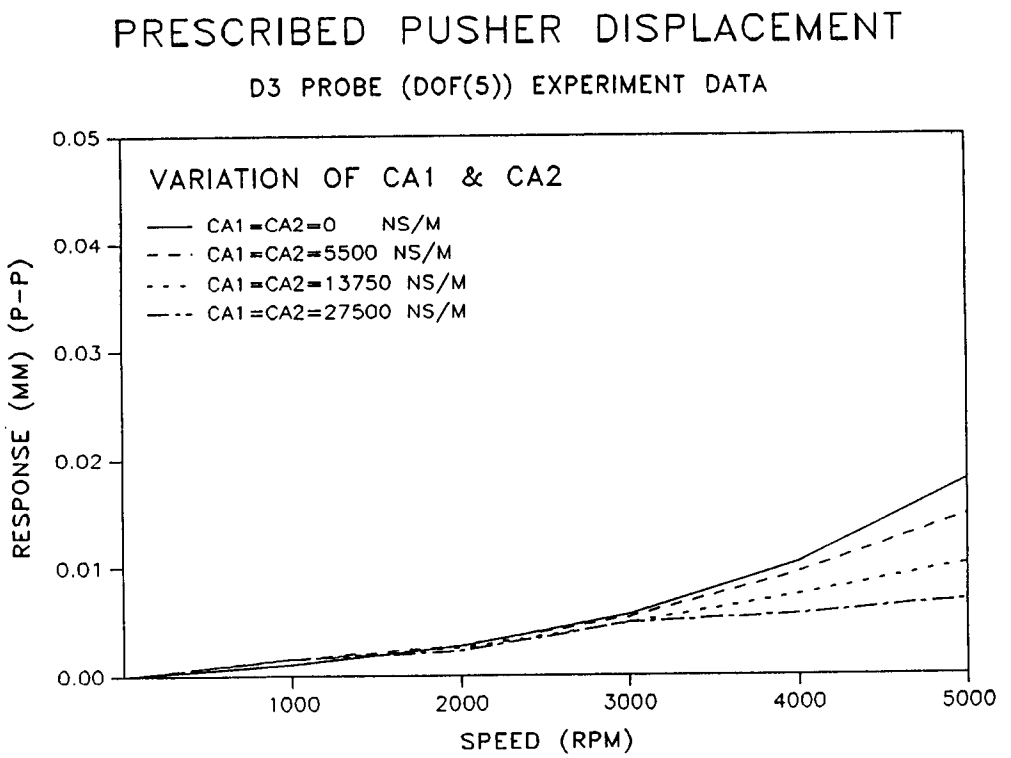

Figure 9 Measured unbalanced response plot at vertical, d_3, probe.

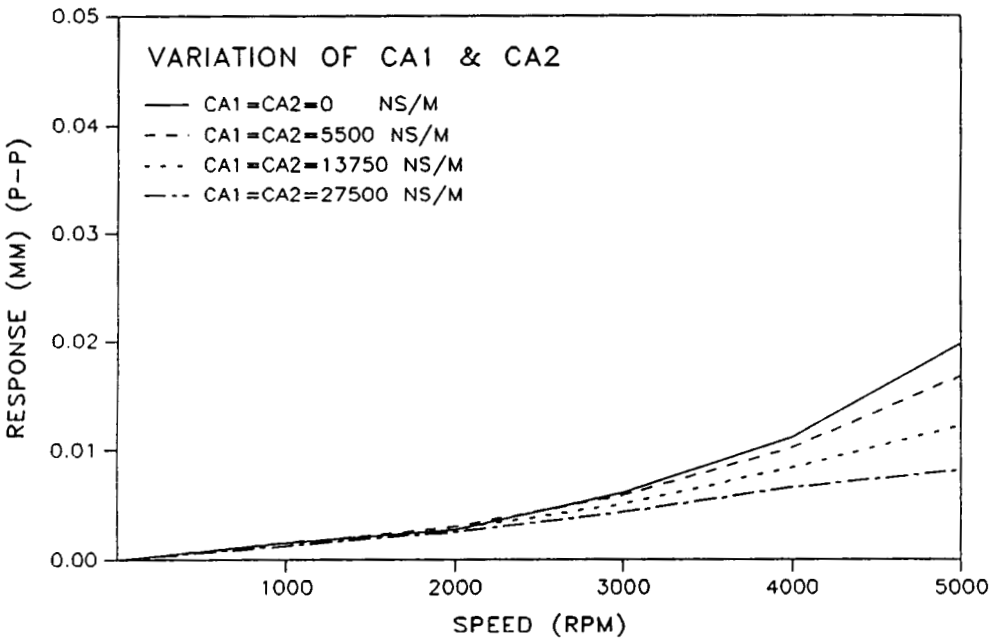

Figure 10 Measured unbalanced response plot at horizontal, d_4, probe.

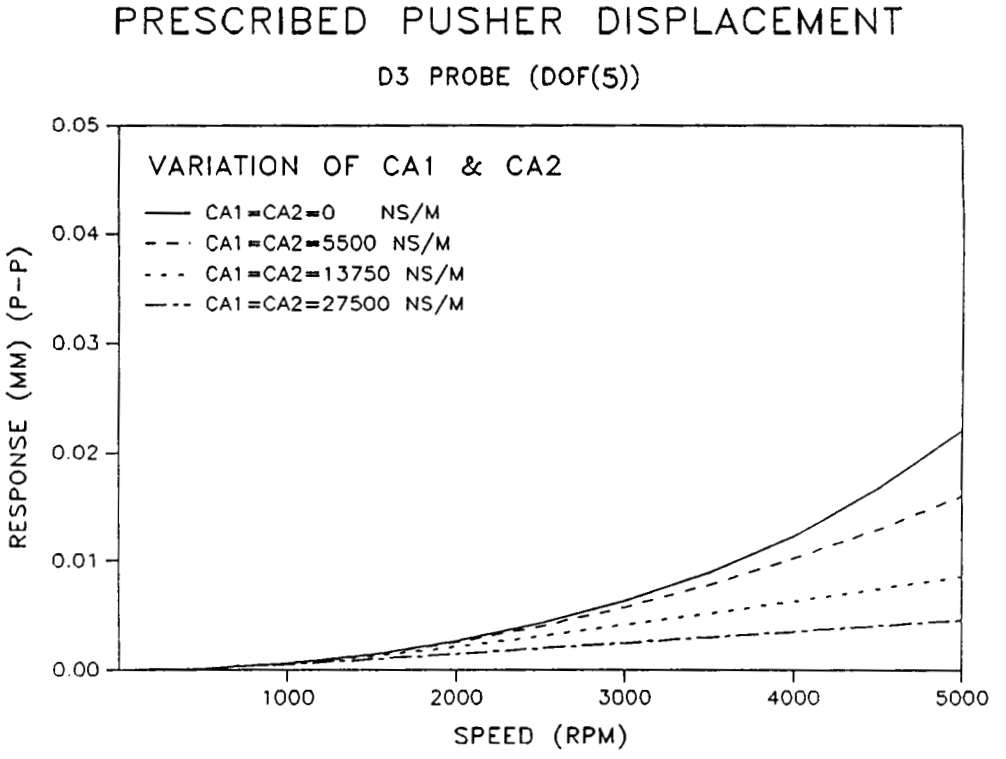

Figure 11 Computer simulation (theoretical) predicted response at probe d_3.